5-27-1970

The modulation of sine-wave gratings at Fourier and Fresnel imaging points

Donald Kingsley

THE MODULATION OF SINE-WAVE GRATINGS AT FOURIER AND FRESNEL IMAGING POINTS

by

Donald M. Kingsley III
Captain, U.S. Air Force

This thesis is submitted in partial fulfillment of the requirements for a Master of Science degree in Photographic Science at the Rochester Institute of Technology.

Accepted by:
John F. Carson, Thesis Advisor 5/27/70
Burt H. Carroll
A. Rickmers

ACKNOWLEDGEMENT

I take this opportunity to thank my thesis advisor Professor John Carson of the Department of Photographic Science, Rochester Institute of Technology for his patience and assistance without which I could never have completed this paper. I would like also to thank Mr. Donald Lehmbeck of the Xerox Corporation for suggesting the topic of the experiment.

ABSTRACT

When illuminated by a coherent light beam, a periodic object will be imaged in near-field space at predictable intervals. This phenomenon is termed self imaging. Recordings of the intensity distribution of sine-wave gratings were made at several positions behind the gratings. The modulation of the images was calculated and used as a predictor of distance from the grating. Positional accuracies of one part in one-hundred fifty-eight were obtained.

I. INTRODUCTION

If a beam of coherent, monochromatic radiation strikes a periodic object, a series of identical images of the object will be formed at predictable distances from the object. Some experimenters have termed this phenomenon self imaging because an image-forming device is not needed to produce the images. The self-imaging effect has been known for many years (1) and the formula which predicted the position of the images was first developed by Lord Rayleigh in 1881(1). Many people have addressed themselves to the mathematical prediction of diffraction patterns in the near field or Fresnel region. Hopkins(2) in 1953 produced a classic paper which described the properties of image-forming systems. In 1957, Cowley and Moodie produced a series of papers (3) which treated the general case of self imaging and determined the specific mathematical relationship of wavelength and the period of an object to an imaging point. They called the points of actual reproduction Fourier image points and the intermediate points Fresnel image points. Recently Winthrop and Worthington(4) examined the Fresnel image points both experimentally and theoretically, and Montgomery(5) has done theoretical work examining self imaging in various types of objects. Rogers (6) has produced a computer program which predicts and plots the two dimensional intensity pattern of a line grating and also a hexagonal array of points. An examination of the available literature has produced no evidence of experiments relating to a determination of a quantity which is useful in discriminating the Fourier image point.

The objective of this experiment is to examine the field behind a sinusoidal grating illuminated by a monochromatic plane wave. The intensity of the images which are formed will be recorded at specific distances from the grating and the modulation will be computed. Modulation will be evaluated as a quantity useful in predicting the distance from the original grating. In order to experimentally verify the theoretical considerations, it is necessary to generate gratings free from secondary harmonics.

II. THEORETICAL CONSIDERATIONS

The description of the self-imaging phenomena can be approached from two mathematical viewpoints. The first is the Fresnel-Kirchoff integral, or the Rayleigh-Sommerfeld modification of the Fresnel-Kirchoff integral, which treats a light wave as a scalar. This method assumes that the aperture is large compared to the wavelength and that the diffracted fields are not interpreted close to the aperture(7). The second approach, which also assumes that a light wave can be described by scalar equations, defines a so-called angular spectrum of plane waves which arise from the Fourier analysis of a complex field function interacting with a plane or set of planes(7). The calculation of the field amplitude can be obtained by a Fourier analysis of the complex wave function across the plane(s). The following presentation treats these two approaches in some detail.

Raleigh-Sommerfeld Diffraction Integral

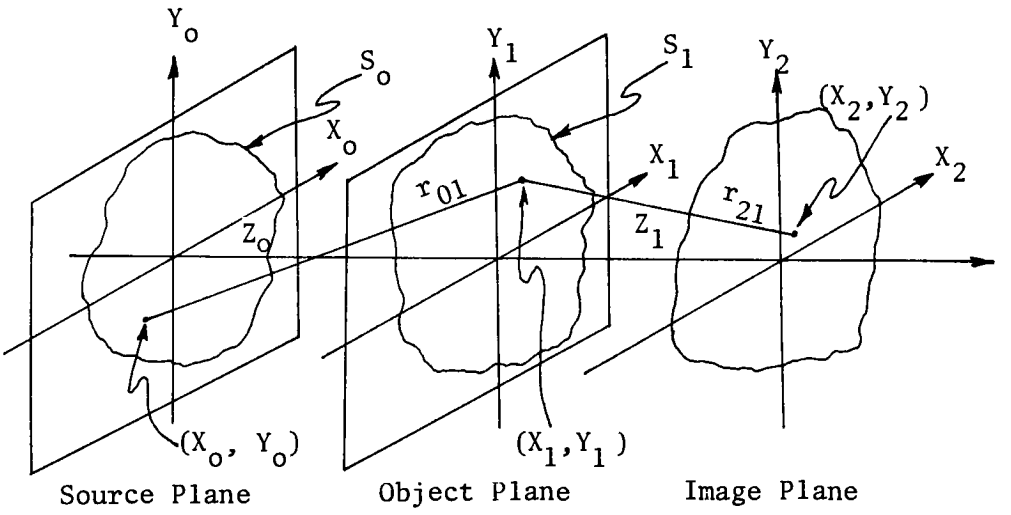

Figure 1. A Coherently Illuminated Periodic Plane

Using the coordinate system established in Figure 1, the formal approach to the theoretical treatment of the problem can be stated. The coherent source lies on a plane at a distance z_o, parallel to the object plane, and is defined by the coordinates of (x_o,y_o). $\bar{r}_{01}$ is the vector from (x_o,y_o) to a point (x_1,y_1) on the object plane. The observation plane lies a distance z_1 from the object plane and (x_2,y_2) is a point on the observation plane where the vector from (x_1,y_1) intersects the observation plane.

If it is assumed that the source is the point (x_o,y_o) and that the object plane has an aperture S_1, then the wave function at (x_2,y_2) can be written in the form of the Rayleigh-Sommerfeld integral(16),

$$u(x_2,y_2) = [i\lambda]^{-1} \int_{s_1} (r_{01}\ r_{21})^{-1} \exp[ik(r_{01}+r_{21})] \cos\ (\bar{n},\bar{r}_{21})ds_1,$$

where $\bar{n}$ is the unit normal, ds_1 is a surface element in the aperture, $\cos\ (\bar{n},\bar{r})$ is an obliquity factor defined as the cosine of the angle between the normal $\bar{n}$ and the vector $\bar{r}$, and k is $2\Pi/\lambda$. The aperture is replaced by a periodic object(3) with amplitude transmission characteristics defined by

$$t(x_1,y_1) = \sum_{hk}\sum T_{hk}\cos[2\Pi\frac{x_1}{a_h} + 2\Pi\frac{y_1}{b_k} + \phi_{hk}],$$

where T_{hk} is the amplitude transmission, and a_h and b_k are the periods of the component waves. In addition, if the source is described by a function $u(x_o,y_o)$ bounded by S_o, the wave function becomes

$$u(x_2,y_2) = [i\lambda]^{-1} \int_{s_o}\int_{s_1} t(x_1,y_1)\ u(x_o,y_o)\ (r_{01}\ r_{21})^{-1}$$

$$\exp[ik(r_{01}+r_{21})]\ \cos(\bar{n},\bar{r}_{01})\ \cos\ (\bar{n},r_{21})\ ds_o ds_1$$

where ds_o is a surface element on the source. To simplify this equation for integration, it is assumed that the distance z_1 from the object plane to the image plane will be much larger than the maximum values of (x_1,y_1); it is also assumed that the aperture is much smaller than z_1. From these

two premises the obliquity factor approaches 1, or $\cos(\bar{n},\bar{r}_{21})\simeq 1$ (7). Similar reasoning can be applied to the $\cos(\bar{n},\bar{r}_{01})$ term(8). If the integration is limited to one dimension along the x_1 axis, and $u(x_o,y_o)$ is assumed to be a point source on the z_o axis, the integral becomes

$$u(x_2) = [i\lambda]^{-1} [r_{01}\ r_{21}]^{-1} u(x_o) \int_{s_1} t(x_1) \exp[ik(r_{01}+r_{12})]dx_1.$$

The distances r_{01} and r_{21} can be approximated by a power series because the linear dimensions of the aperture were assumed to be small in comparison(8). If all constant terms (K) are grouped, and the integration is performed, the equation for the amplitude transmission is

$$u(x_2) = K\Sigma_i \exp[i\nu_i^2]\ T_i\cos\psi_i,$$

where

$$\nu_i = \frac{\pi\lambda}{a_h^2}\left(\frac{z_o\ z_1}{z_o+z_1}\right),\quad \psi_i = \frac{2\pi}{a_h}\left(\frac{z_o}{z_o+z_1}\right)x_2.$$

The intensity transmission, $I(x_2)$, is found from $u(x_2)u^*(x_2)$, and therefore

$$I(x_2) = K^2[\Sigma_h T_h^2\cos^2\psi_h + \Sigma\Sigma_{ij} T_i\ T_j \exp[i(\nu_i^2 - \nu_j^2)]\ \cos\psi_i\cos\psi_j].$$

If $\cos(\nu_i^2 - \nu_j^2) = 1$, the intensity represents an amplitude distribution $u = K\Sigma_h T_h\cos\psi_h$ which is equal to the original amplitude distribution with the exception of a magnification term included in K,

$$M = 2\left[\frac{z_o\ z_1}{z_o+z_1}\right].$$

If from the previous considerations a set of image planes can be defined by allowing ν^2 to equal 2Π, the original object will be imaged at periodic intervals defined by

$$\nu^2 = \frac{\Pi\lambda}{a^2}\left[\frac{z_o\ z_1}{z_o+z_1}\right] = \frac{m_{ij}}{h_i^2-h_j^2}\quad (\text{a set of integers (n)}),\ \text{and}$$

finally,

$$\frac{\lambda}{2a^2n} = \frac{1}{z_o} + \frac{1}{z_1}.$$

If z_o is allowed to become very large as in the case of a plane wave, the magnification term no longer has an effect, and the expression for the self-imaging positions is described as

$$z_1 = \frac{2a^2 n}{\lambda} .$$

If $n = n+\frac{1}{2}$, the intensity distribution is

$$I(x_2) = K^2[\sum_h T_h \cos\psi_h - \sum\sum_{ij} \cos\psi_i \cos\psi_j],$$

the amplitude distribution due to the grating is

$$u(x_1) = K_h \sum_h (-)^{|h|} T_h \cos\psi_h,$$

the original shifted in spatial phase by π.

It has been shown that if a sinusoid grating is illuminated by a coherent light beam, an equation can be formed which will predict points of imaging which contain identical images of the original. If the value of n is not assumed to be an integer value, the original cosine distribution will be imaged along the z-axis but modified by a cosine term which is dependent on the distance from the original grating, the wavelength of the source, and the period(s) of the original grating.

The Angular Spectrum of Plane Waves

The disturbance caused by the interaction between a coherent, plane wave and a periodic grating can be described as a series of plane waves which are mathematically represented by a Fourier series expansion(7). If the grating in Figure 2 is illuminated by coherent, plane wave fronts traveling to the right parallel to the z-axis, the transmittance of the grating can be described by a Fourier series (1),

$$t(x) = \sum_{n=-\infty}^{\infty} a_n \exp[2\pi i n f x]$$

where t(x) is the grating transmittance, f is the grating frequency, and a_n is the wavefront amplitude.

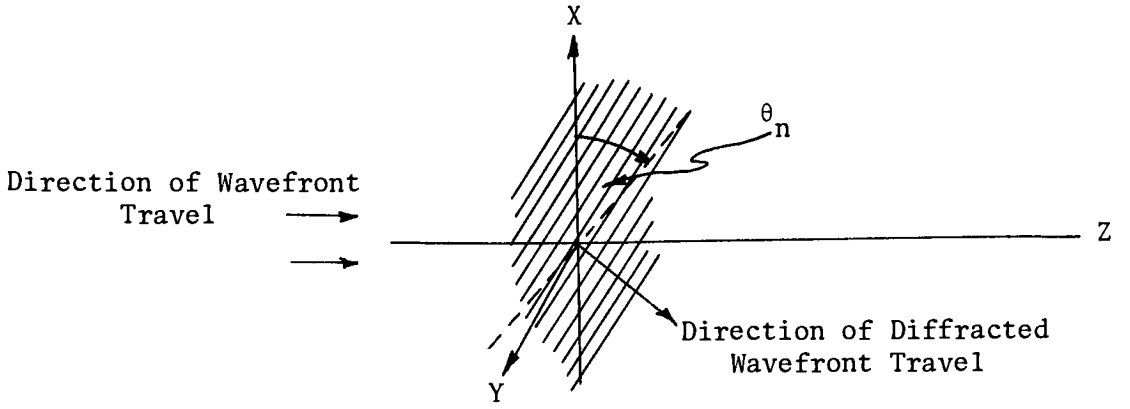

Figure 2. Diffraction at a Screen

The grating transmittance can also be expressed as an angular spectrum of plane waves having the amplitude a_n and propagation angles of θ_n as shown in Figure 3.

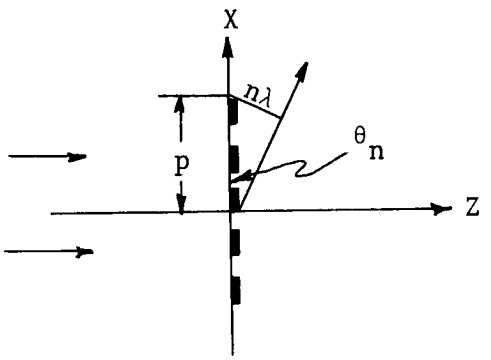

$$\sin \theta_n = \frac{n\lambda}{p}$$

$$= n\lambda f$$

Figure 3. Angular Spectrum

The grating period is p, and λ is the wavelength of the illumination. The amplitude in a plane parallel to the x-y plane at a distance z can be obtained by summing the individual plane wave fronts which were modified by the complex amplitude transmission of the grating to form

$$t(x,z) = \exp(2\pi i\lambda^{-1}z) \sum_{n=-\infty}^{\infty} a_n \exp(-\pi i n^2 \lambda f^2 z).$$

The intensity transmission is the amplitude times its complex conjugate. Assuming that the grating is amplitude modulated and symmetrical about the x-axis, an expression for the intensity pattern at any point on the z-axis can be obtained as follows(1),

$$T_m(z) = \sum_{n=-\infty}^{\infty} a_{m+n}\, a_n \cos(\pi\lambda(m^2 + 2mn)f^2 z);$$

m denotes the mth coefficient of the Fourier series.

If a grating with similar amplitude transmission characteristics as in the previous section is substituted into $T_m(z)$, the intensity at any point along the z-axis can be found. If the grating transmission t(x) is represented by

$$t(x) = \cos 2\pi fx,$$

and the intensity transmission is $\cos^2(2\pi fx)$, the coefficients a_1, a_{-1} will equal ½, all others being zero, and from $T_m(z)$ the transmission is

$$T_o(z) = \tfrac{1}{2}$$

$$T_1(z) = T_{-1}(z) = 0$$

$$T_2(z) = T_{-2}(z) = \tfrac{1}{4}$$

$$T_n(z) = 0 \quad |n| > 2.$$

Thus the intensity distribution at any distance from the grating is

$$T(x,z) = \tfrac{1}{2} + \tfrac{1}{2} \cos 2(2\pi fx) = \cos^2(2\pi fx),$$

which is the same as the original intensity pattern.

Because a grating with zero bias is not a realistic model for the experiment, it is more useful to use a grating with transmission characteristics similar to

$$t(x) = \tfrac{1}{2}(1 + \cos 2\pi fx),$$

whose Fourier coefficients are $a_o = \tfrac{1}{2}$, $a_1 = a_{-1} = \tfrac{1}{4}$. Substitution of these values into $T_m(z)$ gives coefficients of

$$T_o(z) = 3/8,$$

$$T_1(z) = \tfrac{1}{4} \cos \pi \lambda f^2 z,$$

$$T_2(z) = 1/16,$$

and the intensity distribution along the z-axis becomes

$$T(x,z) = 3/8 + \tfrac{1}{2} \cos(\pi \lambda f^2 z) \cos(2\pi fx) + 1/8 \cos 2(2\pi fx).$$

If the z-axis cosine value is 1, the resulting function will follow the curve shown in Figure 4. The implication of the equation for the intensity transmission of this grating is that the image modulation will vary along the z-axis as the cosine of $\pi \lambda f^2 z$ if the term $1/8 \cos 2(2\pi fx)$ is neglected.

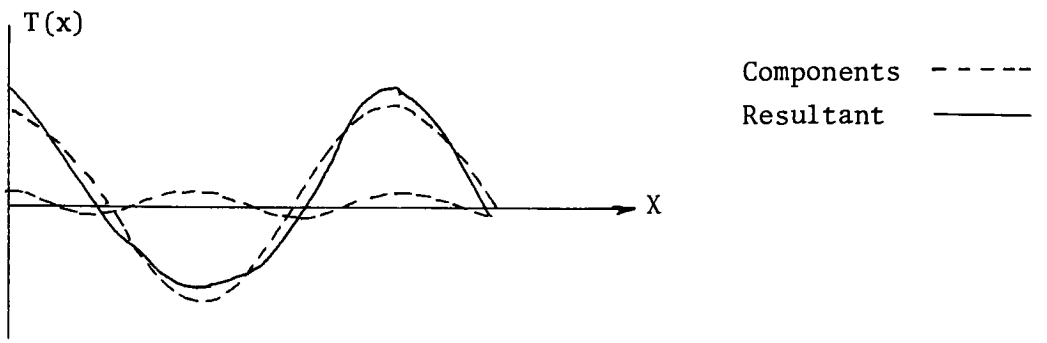

Figure 4. Intensity Distribution

If $1/8 \cos(4\pi fx)$ can indeed be assumed to be very small that is, $<<1$, the modulation in the image will be identical to the modulation in the grating times a cosine term which is dependent on z, λ, and f^2. There will be points at which the modulation approaches zero, and there will be points at which a duplicate of the original appears possibly shifted in spatial phase. The frequency of appearance of this duplicate image, or self image, is defined by setting the cosine argument equal to 2π; the self-imaging period is now defined by $2/\lambda f^2$. The frequency of the grating and the wavelength of the illumination thus determine the distance along the z-axis at which self images occur. It will be shown that the assumption that the righthand cosine term is negligible is valid. From the preceding considerations the question regarding the objective of this thesis remains; can the modulation of the image be measured with sufficient accuracy to determine the z-axis position?

III. EXPERIMENTAL

Production of Sinusoidal Gratings

Sensitometry

The gratings for this experiment must be sinusoidal in amplitude transmission in order to satisfy the original conditions defined by the theory. Photographic film records the intensity of a light wave which is proportional to the square of the amplitude (9). Classically, the reaction of film to light is described by the Hurter and Driffield (H and D) curve (10). The density (D) of the developed image is defined as the log of the reciprocal of the transmission (T), that is, $D = \log (1/T)$; the transmission is the ratio of the transmitted light flux to the incident flux. The equation most commonly used is $D = -\log T$. The H and D curve of photographic materials follows the characteristic shape shown below:

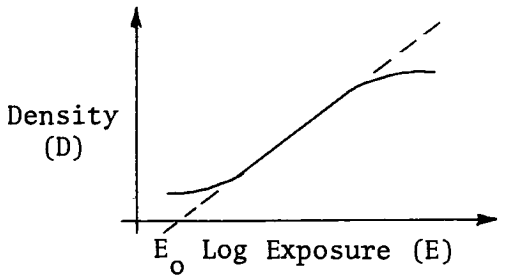

In this case E is the exposure which is equal to the intensity of the illumination multiplied by the time of the exposure; E_o is the point where the tangent to the straight portion of the H and D curve (when it exists) intercepts the log E axis. From the diagram, an expression can be written for the tangent line: $D = \gamma(\log E - \log E_o)$, where gamma ($\gamma$) is the slope of the curve defined as $\Delta D/\Delta \log E$. Because $D = -\log T$, the curve equation can be rewritten as: $-\log T = \gamma(\log E - \log E_o)$ or:

$$T_I = \left[\frac{E}{E_o}\right]^{-\gamma}.$$

This expression is the intensity transmission (T_I) of the transparency. If phase effects introduced by the film are neglected, the amplitude transmission (T_A) can be obtained by taking the square root of T_I, that is, $T_A = \left[\frac{E}{E_o}\right]^{-\gamma/2}$. It is apparent that in order to maintain amplitude transmission proportional to exposure, γ must equal -2.

Ordinarily to obtain a γ of -2, it is necessary to reversal process the film or to use a negative-positive process (9). In this case the sinusoid nature of the image could be exploited. If the slope of the characteristic curve is linear over a sufficient portion, the sinusoid grating does not have to be reversal or negative-positive processed. This is best illustrated by the sketch below:

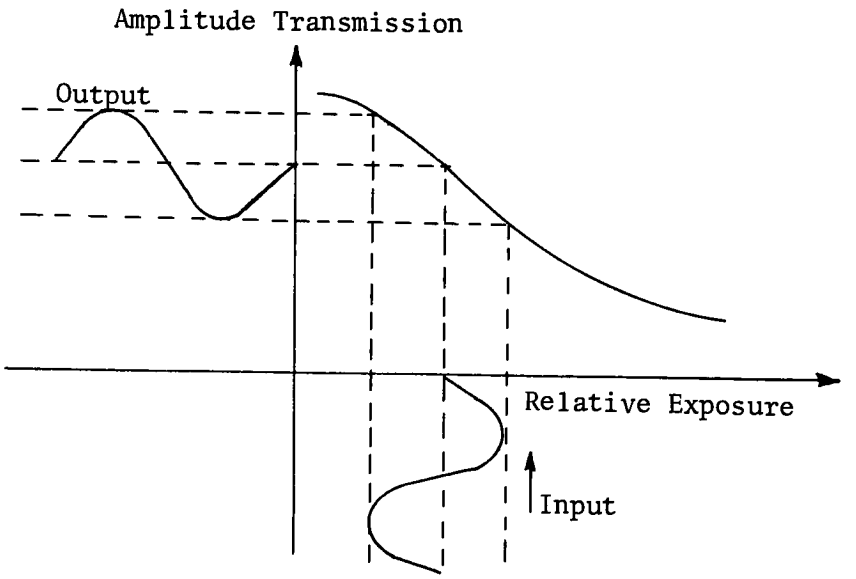

If the characteristic curve of T_A versus exposure is linear, the output wave will be identical in shape to the input, but the phase will be shifted by 180 degrees in space; that is to say the light portion of the input

will be the dark portion of the output and vice versa. This is equivalent to the expression: $\cos(x) = \cos(x+\pi)$. Therefore, because the grating remains a sinusoid, there is no need to reversal process. This rationale was used in the production of the gratings.

Although the distribution of exposure within the emulsion can be a function of spatial frequency, under certain conditions (9), it was assumed that over the range of frequencies used, the film response would be uniform. Phase changes which are introduced by surface deformations of the developed film must also be eliminated. Leith (11) suggests using a liquid gate technique where an emulsion index-matching fluid is placed on the film which is sandwiched between two optical flats. KODAK High Contrast Copy film was selected for fringe recording (see Appendix I). To determine the correct slope, a template with a slope of 2 was made. From the characteristic curves (see Appendix II) it can be seen that these processing conditions produce a fairly constant slope; the development time of 6 minutes was used.

Apparatus

The requirements for the gratings to be used in this experiment were:

a. Uniform grating transmission over an area approximately 24mm x 36mm.

b. Variation of grating frequency from approximately 2c/mm to 100c/mm.

c. Variation of grating modulation.

A method for grating production suggested by Swing and Shinn (12) and also by Leith (11) was examined. The Fourier transform of a Ronchi ruling (R) is taken by a lens (L_1). The resulting orders of diffraction

can be filtered by a spatial filter (SF) and re-transformed by L_2 to produce cosine fringes of varying frequency and contrast (see sketch below).

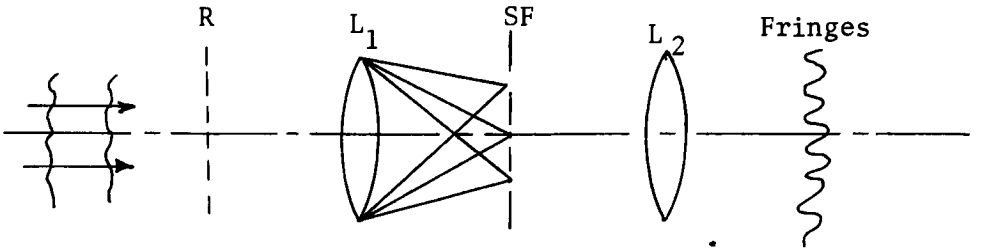

This method was attempted, but the available Ronchi ruling appeared to have a very low spatial frequency envelope of the sort produced when two frequencies beat together. A microdensitometer produced a trace of fringes obtained from the ruling similar to the following sketch.

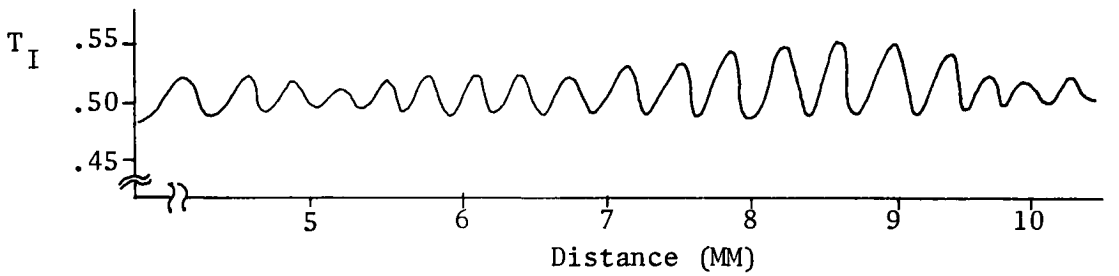

Because this condition would introduce unwanted harmonics and self-images into the experiment, the use of a Ronchi ruling was abandoned.

A second method for making sinusoid gratings is realized by creating interference fringes (see Appendix III). The Twyman-Green modification of the Michaelson two-beam interferometer (8) has features which meet the previously stated requirements. An Ealing, Michaelson interferometer was used with a laser source. A 40x microscope objective (MS) was placed in

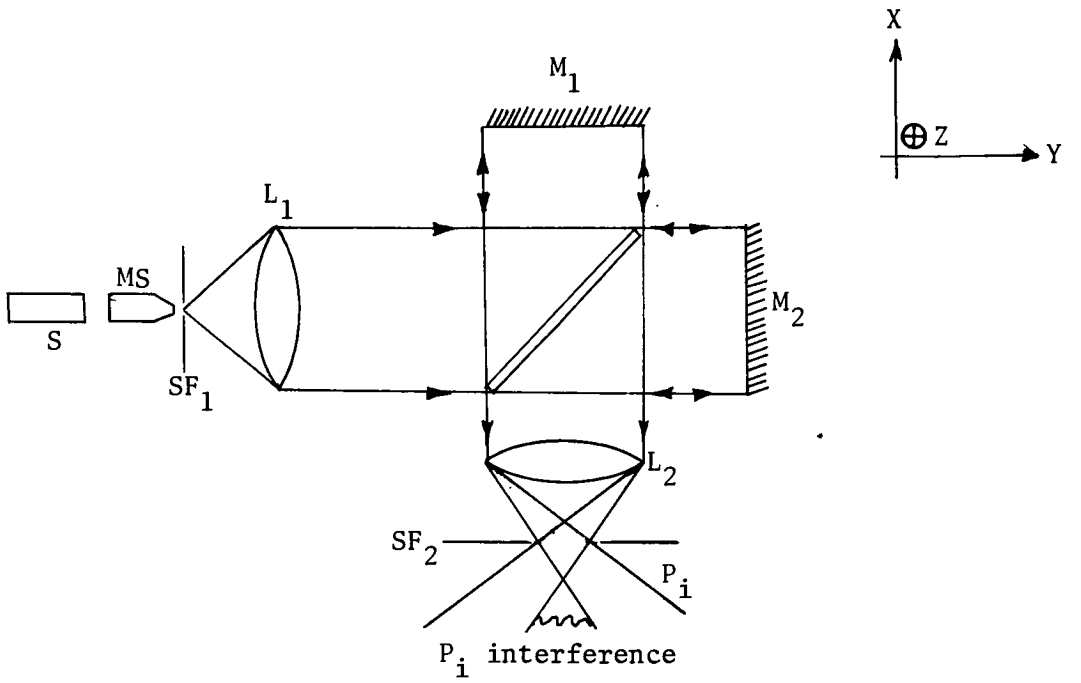

front of the laser (S) and the beam focussed onto a 12.5-micrometer-diameter spatial filter (SF_1). A lens (L_1) collimated the TEM_{oo} mode beam to ±.05 log E, an almost flat beam intensity across the interferometer aperture. Another lens (L_2) brought the fringe pattern to a focus, and the fringe pattern on the opposite side of this focal point was extensive enough to fill a 35mm negative. The fringe frequency was varied with a micrometer screw by tilting the mirror, M_1, either about the Z-axis or Y-axis.

Steel (13) describes the problems involved in replacing a conventional source with a laser in an interferometer. The reflections created by each optical surface will form additional, unwanted fringe

patterns due to the characteristic long coherence length. In this case four reflections of the source were observed at the focus of L_2. The dot array could be varied by tilting the reference mirror (M_1) either along its vertical or horizontal axis to create either a parallel set of unwanted fringes or a cross hatch at the image plane (P_i) (see below).

A Brewster's angle beam-splitter would reduce these reflections when used with the polarized light beam from the laser. Because of mechanical limitations on the interferometer, a Brewster's angle beam-splitter could not be installed. L_2 transformed the four reflections to frequency space, and a spatial filter (SF_2) was introduced at the focus of L_2 eliminating the unwanted orders. A suitably sized pinhole was placed at the image plane and the two unwanted points were removed (see sketch).

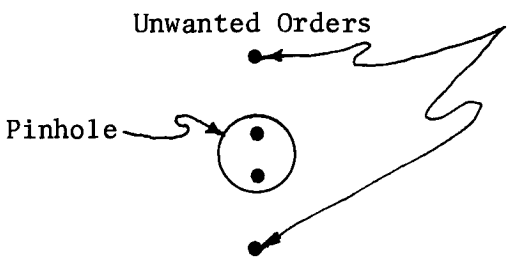

A Nikormat camera body was set up behind the spatial filter to record the fringes. The filtered fringes which were of uniform intensity, free from spurious images, and of sufficient size to fill the film plane were then recorded.

Gratings

The biasing of the fringes to control modulation was accomplished by cutting off one beam of the interferometer and fogging the film with a pre-exposure of 0.1 second. The fringe exposure time was varied. The density of the grating was measured by a macro-densitometer to determine where the average exposure was located on the T_A vs E curve. When the correct exposure was determined, several gratings were made, and a Fourier transforming setup (11) was assembled on the optical bench to check for the presence of unwanted harmonics introduced by emulsion thickness variations. The diffraction pattern of the gratings was examined with a microscope, and in all cases an unwanted second order point existed. Several iterations of exposure and processing were performed, but it appeared as though the film were introducing a phase change. To eliminate this change, an index-matching liquid was made by mixing together Cargille Immersion Liquids of 1.624 and 1.457 refractive index in a 1:1 ratio to produce an index of approximately 1.540 (14). The film was coated with the fluid and sandwiched between two optical flats. The unwanted side order disappeared completely, and the gratings were produced. Ten gratings were generated with bias and frequency ranges as shown in Table 1.

TABLE I

BIAS AND FREQUENCY RANGES

	Frequency (c/mm)	Bias Exposure (sec)	Fringe Exposure (sec)
f_1	1.74	0.1	0.1
f_2	4.14	0.1	0.1
f_3	4.53	0.1	0.2
f_4	4.53	0.1	0.04
f_5	9.45	0.1	0.1
f_6	11.80	0.1	0.2
f_7	11.80	0.1	0.04
f_8	18.45	0.1	0.1
f_9	26.95	0.1	0.1
f_{10}	32.70	0.1	0.1

The determination of the grating frequency was made by counting fringe peaks recorded by the slit-scanning photometer. A spatial interval large compared to the grating period was used to average the period.

Experimental Procedures

The modulation measurement apparatus was mounted on a Tech Ops 3-metre optical bench. A microscope (M) of 100x magnification and a phototube housing (PT) with a variable slit were mounted together on a single plate to ensure constant magnification. Precision micrometer screws (MS) accurate to 0.0005 inches, ±0.0002 inches, were attached to the plate for positioning in the x- and z-axes as shown below.

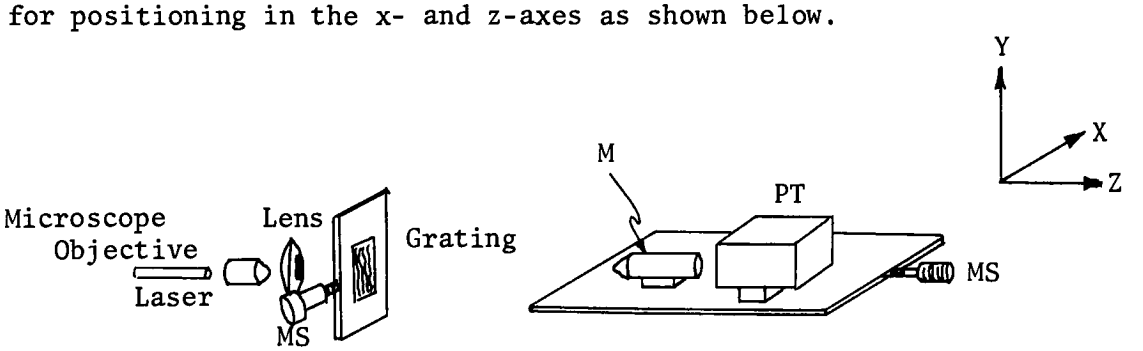

Experimental Set-Up

The slit width was varied between 0.3mm and 1.5mm depending on the fringe frequency. This aperture was sufficient to ensure that the slit was small relative to the grating period (approximately 10:1, period to slit size). Each self-imaging period was divided into ten positions along the z-axis, and the image at each position was scanned by moving the target with a synchronous motor along the x-axis for approximately 0.1 in. The microphotometer apparatus was then moved to the next position on the z-axis and a new reading was made. The phototube output was amplified by an Amnico photomultiplier amplifier and recorded by a Varian Associates G-11A Strip Chart Recorder. After each intensity measurement was recorded, the photomultiplier and strip chart were re-zeroed. It was necessary to allow the gratings to stand for a while after the liquid gate was made to let excess liquid bleed from between the plates. If this did not occur, changes in transmission would occur as the liquid moved between the plates.

To establish the validity of the measurement apparatus, the modulation of each grating, the square root of two times the ratio of the side order to the central order, was determined from measurements made by a Fourier transforming apparatus set up on the optical bench. Measurements of the central and side orders were made in the spatial domain as suggested by Leith (11) (see below).

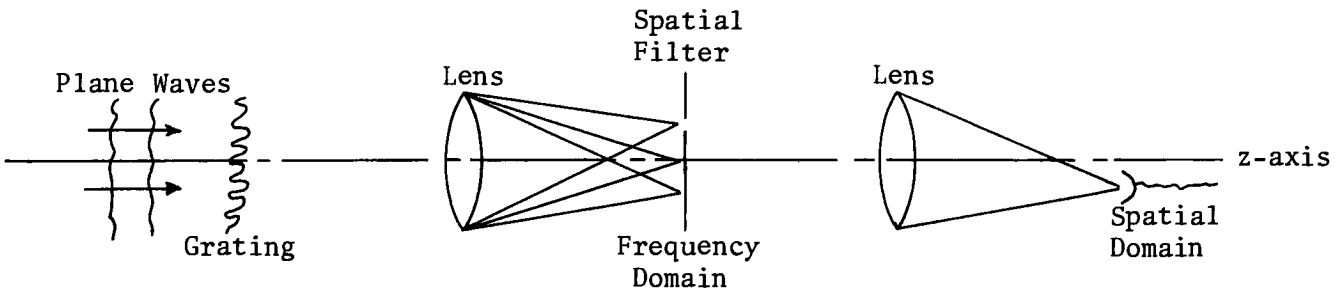

Fourier-Transforming Apparatus

Care was taken to ensure that the same area on the grating used for the sinusoid traces was used for modulation measurement. The amplitude transmission of the gratings was computed from the intensity measurements and then the modulation was determined. The results are shown in Table II.

TABLE II

GRATING PARAMETERS

Bias (sec)	Grating (Amplitude Transmission)
0.1	$0.223(1+0.281 \cos 2\pi f_1 x)$
0.1	$0.200(1+0.245 \cos 2\pi f_2 x)$
0.2	$0.200(1+0.141 \cos 2\pi f_3 x)$
0.04	$0.200(1+0.212 \cos 2\pi f_4 x)$
0.1	$0.200(1+0.200 \cos 2\pi f_5 x)$
0.2	$0.223(1+0.245 \cos 2\pi f_6 x)$
0.04	$0.314(1+0.284 \cos 2\pi f_7 x)$
0.1	$0.223(1+0.200 \cos 2\pi f_8 x)$
0.04	$0.314(1+0.156 \cos 2\pi f_9 x)$
0.04	$0.314(1+0.142 \cos 2\pi f_{10} x)$

Next, the modulation of the images was found from estimates of the average maximum and minimum of the chart recordings. These modulation values were compared to the modulations obtained from the results of the Fourier transforming operation. A scatter diagram was drawn, and the correlation coefficient was calculated (Appendix IV) and found to be significant. The significant correlation indicates that the slit-scanning experimental technique was valid and is a good method for measuring the modulation of the targets. A plot of a typical modulation-vs-position curve is presented in Appendix V. A graph of actual test traces versus a photograph of the image is presented in Appendix VI. A computer program was written to normalize the individual modulations and plot them as a function of $\lambda f^2 \pi z$ (see Appendix VII).

Conclusions

Each modulation was normalized to the highest modulation of the individual target to obtain some estimate of experimental error. Because the data should follow a cosine distribution, several methods to determine the best fit curve through the data were tried. In each case the cosine-squared term was assumed not to be significant. This assumption can be considered valid when the actual values of the terms are considered. The values averaged 0.05 transmission units or less and were thus below the sensitivity of the photomultiplier-chart recorder combination.

The normalized data (modulation vs $\lambda f^2 \pi z$) was evaluated by a nonlinear regression analysis program (See Appendix VIII). A cosine curve was fit to the data, and precision terms were calculated for the experimental data. From an analysis of the precision values, it was determined that the maximum error in position, when the position is calculated from the modulation, is one part in one hundred-fifty eight (1:158). This ratio is equivalent to stating that the distance from a 1 c/mm grating, illuminated by 632.8 nm laser light, can be determined to ±20mm over an interval of 3160mm by measuring the modulation. From the theoretical considerations and the results of the analysis of the experimental data it has been shown that modulation of the self images of sinusoidal gratings can be measured accurately enough to predict the spatial distance from the original grating as long as the cycle in which the measurement is being made is known.

REFERENCES

1. R. F. Edgar, Optica Acta, 3, 281 (1969).
2. H. H. Hopkins, Proc. R. Soc., 217, 408 (1953).
3. J. M. Cowley and A. F. Moodie, Proc. R. Soc. B, 70, 486, (1957); Ibid., 70, 497 (1957); Ibid., 70, 505 (1957),; Ibid., 71, 533 (1958).
4. J. T. Winthrop and C. R. Worthington, J. Opt. Soc. Am., 55, 373 (1965).
5. W. D. Montogomery, J. Opt. Soc. Am., 57, 722 (1967).
6. G. L. Rogers, Brit, J. Appl. Phys., 14, 657 (1963); Ibid., 15, 594 (1964).
7. J. W. Goodman, Introduction to Fourier Optics, (McGraw-Hill, Inc., New York, 1968), p. 31.
8. M. Born and E. Wolf, Principles of Optics (Pergamon Press, New York, 1965) p. 302, p. 561.
9. P. F. Mueller and G. O. Reynolds, J. Opt. Soc. Am., 57, 1343 (1967).
10. C. E. K. Mees and T. H. James, The Theory of the Photographic Process (The Macmillan Company, New York, 1967), p. 72.
11. E. N. Leith, Phot. Sci. Eng., 6, 75 (1962).
12. R. E. Swing and M. C. H. Shin, Phot. Sci, Eng., 7, 350 (1963).
13. W. H. Steel, Interferometry (University Printing House, Cambridge, Eng., 1967), p. 167.
14. E. Sklar, Phot. Sci. Eng., 13, 29 (1969).
15. W. F. Voglesong, Eastman Kodak Co., private communication.
16. A. D. Rickmers and H. N. Todd, Statistics: An Introduction (McGraw-Hill, Inc., New York, 1967), p. 239.
17. J. Strong, Concepts of Classical Optics, (W. H. Freeman and Co., San Francisco, 1958), p. 377.
18. System/360 Scientific Subroutine Package (IBM Corp., White Plains, N. Y., 1968).

APPENDIX I

For dimensional stability and fine grain, KODAK 649-F High-Resolution Plates were originally considered. These plates were obtained and the backs were painted with a solution of lamp black and shellac to minimize reflection. A sensitometer was set up using tungsten illumination with a 632.8 nanometer interference filter to approximate the laser light to be used. Vogelsong(15) stated that Kodak results had shown no significant difference between this method and laser sensitometry. He further stated that amplitude measurements could be obtained by taking the square root of intensity measurements derived from macrodensity measurements. A high-quality filter was of course necessary. A Baird Atomic B-1 interference filter with a 9.3nm bandwidth was used. A regression analysis(16) was performed on the results of the 649-F sensitometry and a second-order equation fit to the curve. The result was: Density = 16.54+12.66(Log Exposure)+2.44(Log Exposure)^2. The first derivation showed that a slope of 2 would fall on the toe region which is very low in contrast. Because of the difficulty of lowering the 649-F D-Log E curve to a gamma of 2, it was decided to use a different film.

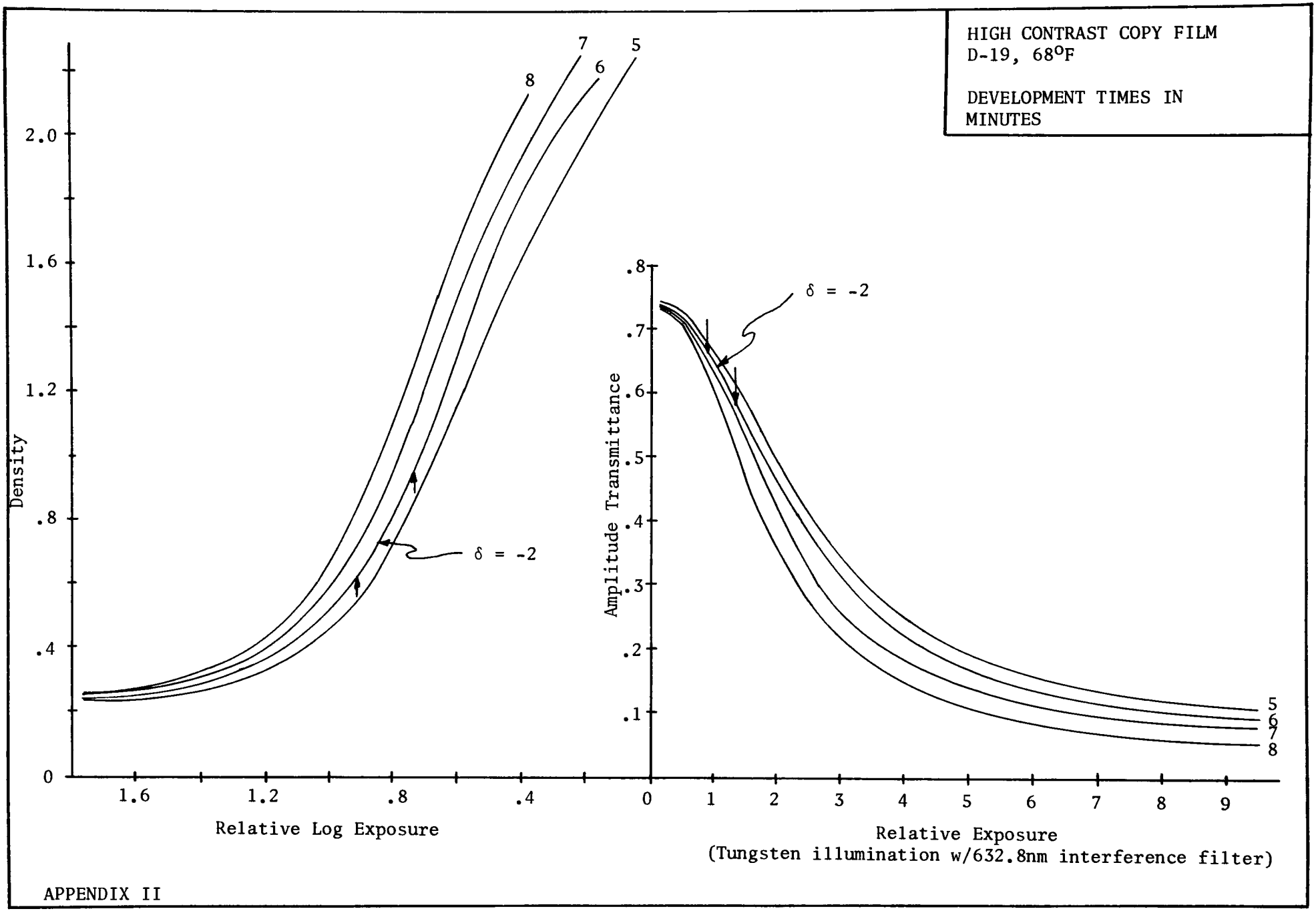
HIGH CONTRAST COPY FILM
D-19, 68°F
DEVELOPMENT TIMES IN MINUTES
Density
2.0
1.6
1.2
.8
.4
0
8
7
6
5
δ = -2
1.6
1.2
.8
.4
Relative Log Exposure
Amplitude Transmittance
.8
.7
.6
.5
.4
.3
.2
.1
δ = -2
5
6
7
8
0
1
2
3
4
5
6
7
8
9
Relative Exposure
(Tungsten illumination w/632.8nm interference filter)

APPENDIX II

APPENDIX III

Two methods of fringe production were tried and rejected: Lloyd's mirror(17), and Young's slit experiment(17). The principle disadvantage of Lloyd's mirror (see below) was the finite area of the fringe pattern.

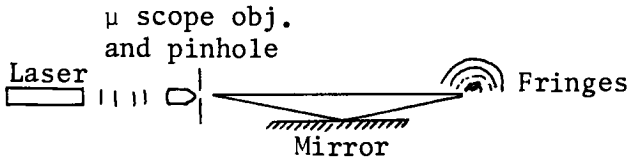

The fringe intensity varied, and the fringes were bounded by the diffraction of the pinhole.

The second method was a modified Young's slit experiment (see below).

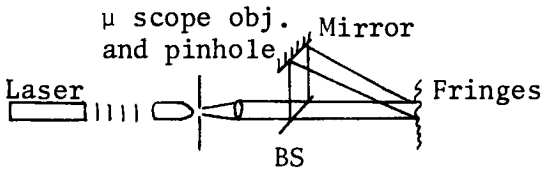

This method was equipment limited because precision slits were not available. Using a beam-splitter, two point sources were created, and fringes were generated, but the small separation necessary for low frequencies could not be achieved. The fringe frequency (200c/mm) was too high and the fringe contrast was too low.

APPENDIX IV
SCATTER DIAGRAM

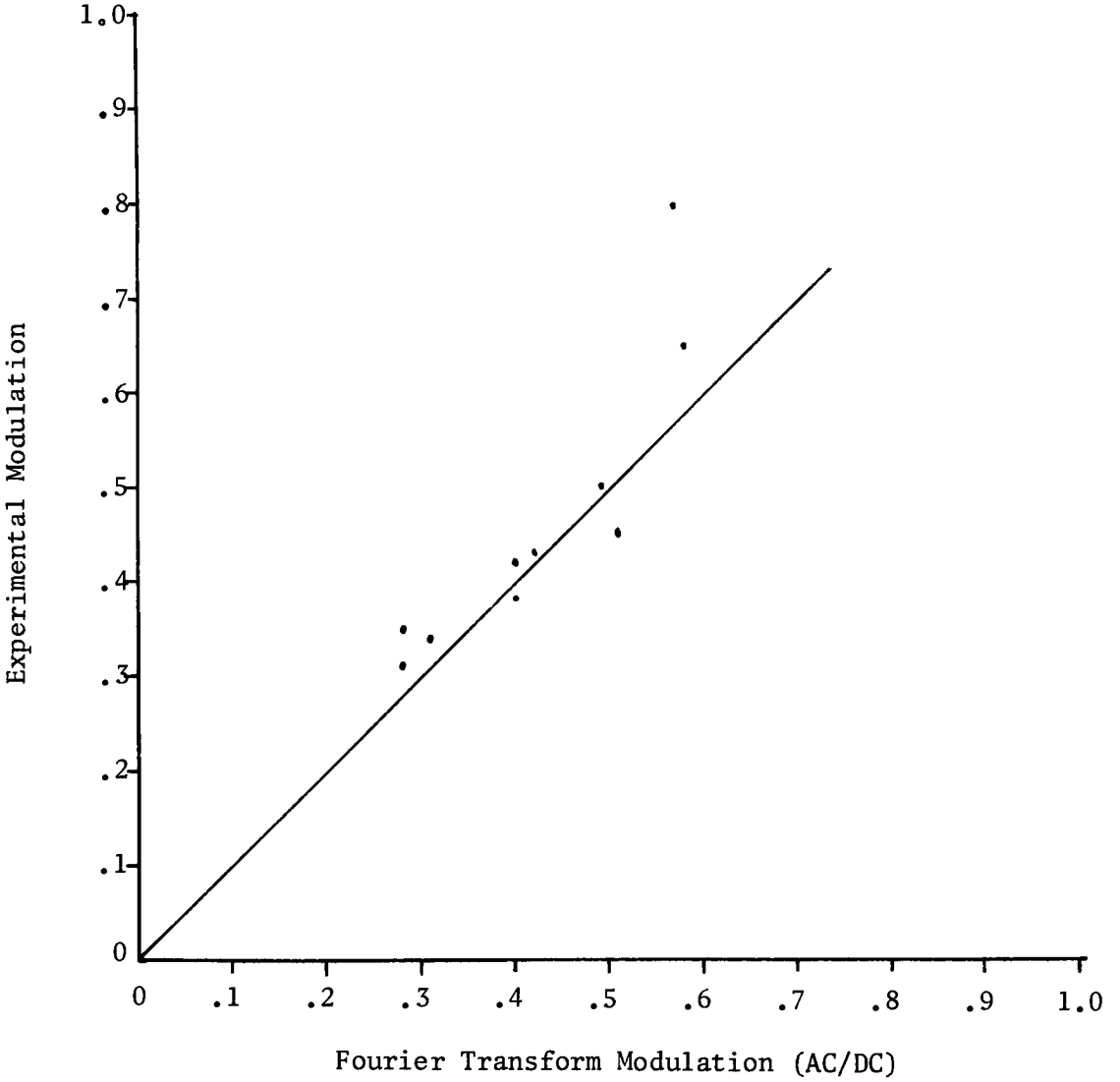

r (Correlation Coefficient) = 0.9878

Any variation in the plot is due to
experimental random factors.

APPENDIX V

SAMPLE PLOT OF MODULATION
GRATING FREQUENCY 26.95c/mm
BIAS = .1 SEC

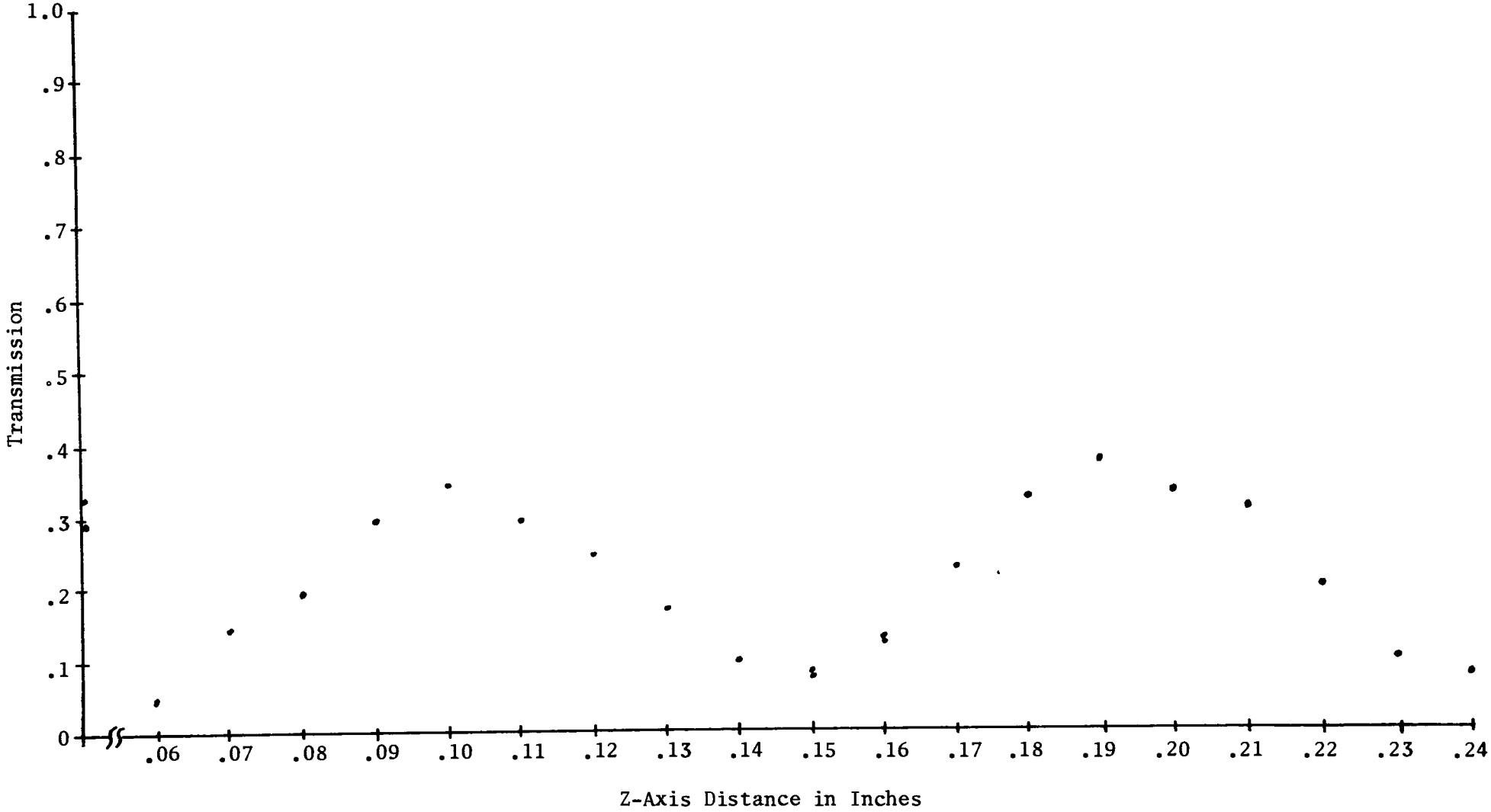

APPENDIX VI

SAMPLE TRACES FOR f = 9.45 c/mm
1.5 IN = 1.89 MM

M is modulation
Imaging period
is 0.800 IN

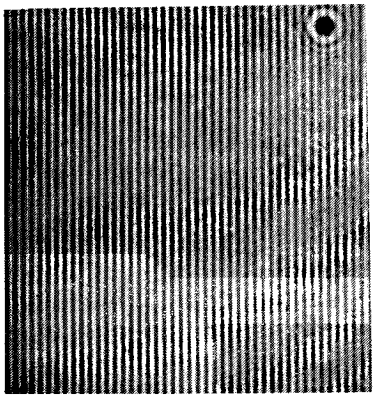

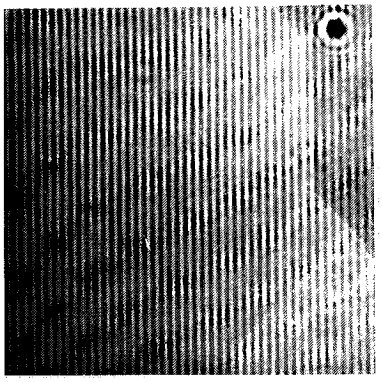

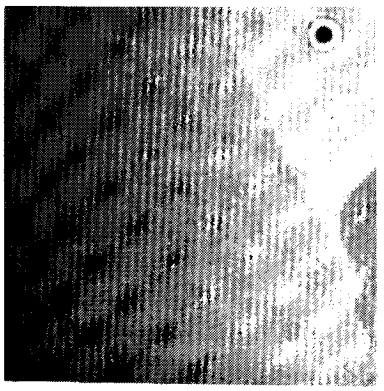

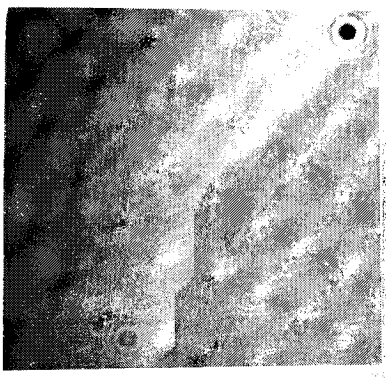

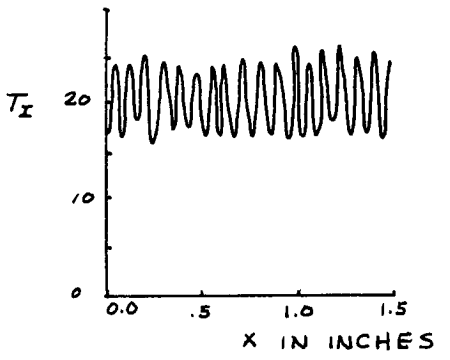

Z = 0.000 IN
M = 0.39

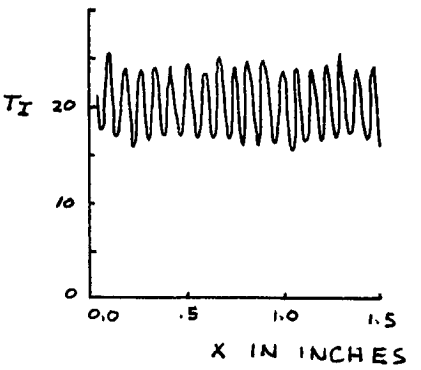

Z = 0.300 IN
M = 0.39

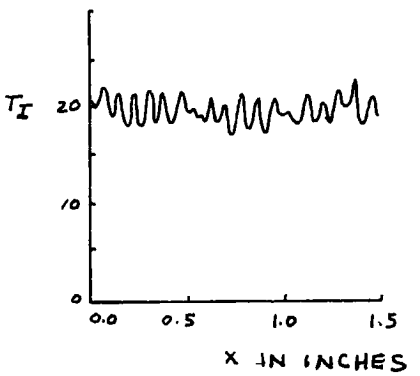

Z = 0.600 IN
M = 0.14

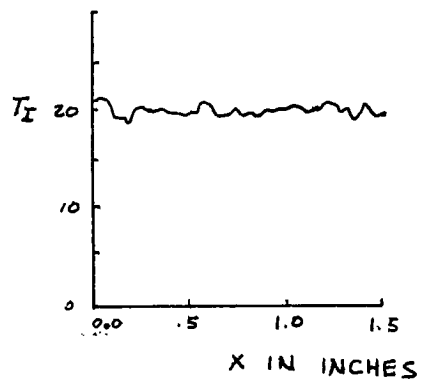

Z = 0.675 IN
M = 0.02

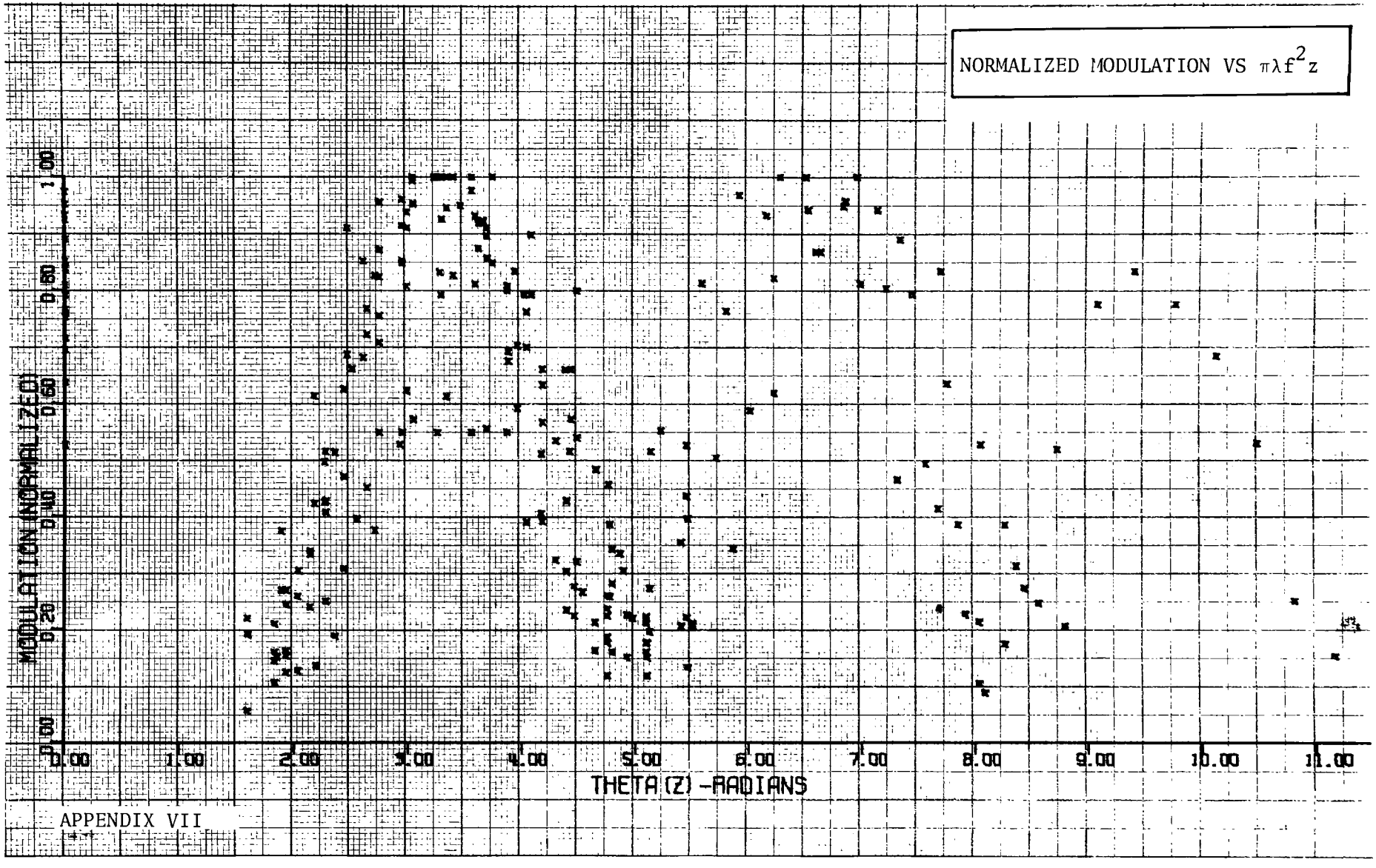

APPENDIX VII

APPENDIX VIII

A Fourier analysis of the data was considered, but because of the random distribution of the data, the Fourier approach was discarded. The data could have been grouped, but this technique may have introduced an unwanted bias into the results. A polynomial regression analysis was performed on the data because the cosine can be expanded by the series:

$$\cos x = 1 - \frac{x^2}{2!} + \frac{x^4}{4!} - \frac{x^6}{6!} + \ldots$$

If the polynomial obtained had very-low odd x powers and followed the general form of the expansion, the data could be assumed to be sinusoidal and an error estimate could be derived. The equation which was calculated by a program in the IBM Scientific Subroutine Package(18) took the following form:

$$Y = 0.77 - 0.59X + 0.35X^2 - 0.076X^3 + 0.005X^4 - 0.0001X^5 - 0.00001X^6$$

This form obviously does not follow the expansion. The values of the cosine computed from this expression were also in poor agreement with the actual data points.

William Lawton, a professional statistician at Eastman Kodak Company, examined the computer plot (Appendix VII) of the normalized data and stated that since a sinusoidal distribution is predicted by the theory, and the data plots sinusoidal, the only analysis he would perform would be a nonlinear regression using a biased cosine with, and without, a phase shift, as the statistical model. A nonlinear regression analysis (Eastman Kodak Company Proprietary Program) was performed by computer. The program calculates bias level, amplitude, frequency, phase, and error terms for each of these parameters. Two curves were fit to the data (Figure VIIIa, b) and the resulting equations of the curves are:

$$Y(t_1) = 0.567 + 0.334 \cos (1.934t - 0.244),$$

$$Y(t_2) = 0.561 + 0.333 \cos (1.888t)$$

where: $Y(t)$ = modulation, and

$Nt = \lambda f^2 \pi z$.

Because the degree of correlation for the curve with phase shift ($Y(t_1)$) is statistically the same (0.850 for $Y(t_1)$ vs 0.856 for $Y(t_2)$), the equation with the phase term was discarded. Using $Y(t_2)$ as the model, error terms were computed for each of the model variables. The results are shown in Table A.

Table A. Error Terms

Variable	Value (95% conf.)	Percent Error (95% conf.)
z-axis modifier(t)	1.890 ±0.022	0.95
DC level	0.560 ±0.019	3.50
Amplitude	0.330 ±0.026	7.90

An analysis of these results indicates that errors arising from positioning inaccuracies along the z-axis or errors arising from the grating frequency measurements are not significant. This aspect of the experiment was statistically in control. The error in the bias level and amplitude terms does not seem large when the method of measurement is considered. A significant error factor in the computation of these terms is the method for normalizing the various modulations. Because each target was normalized against itself, the nonlinear model represents the total error. If a model were fit for each target-modulation series, the term would probably be less; thus, for the selected range of target frequencies and z-axis positions, the modulation can be measured to ±7.9, 95 percent of the time. This inaccuracy corresponds to a modulation, or cosine term error of at most ±0.079 at the maximum modulation of 1.000. This value of the modulation indicates that the Fourier image point can be predicted to ±0.40 radians, or the position error at this point is ±12.5 percent. If the grating frequency error is assumed to be negligible, the z-axis error can be computed by determining the actual z-distance of 0.4 radians from the relation: argument (radians)= $\lambda\pi f^2 z$. If the wavelength is 632.8nm, z becomes $\pm 20.0/f^2$ for 95 percent.

This error can be interpreted for 1 c/mm where the self-image interval is 3160 mm. Thus, if the modulation is measured, the maximum position error at any point would be ±20mm. From these computations it follows that the technique for determining z-axis position using modulation measurements is valid if the cycle in which the measurement is being made is known.

APPENDIX VIIIa

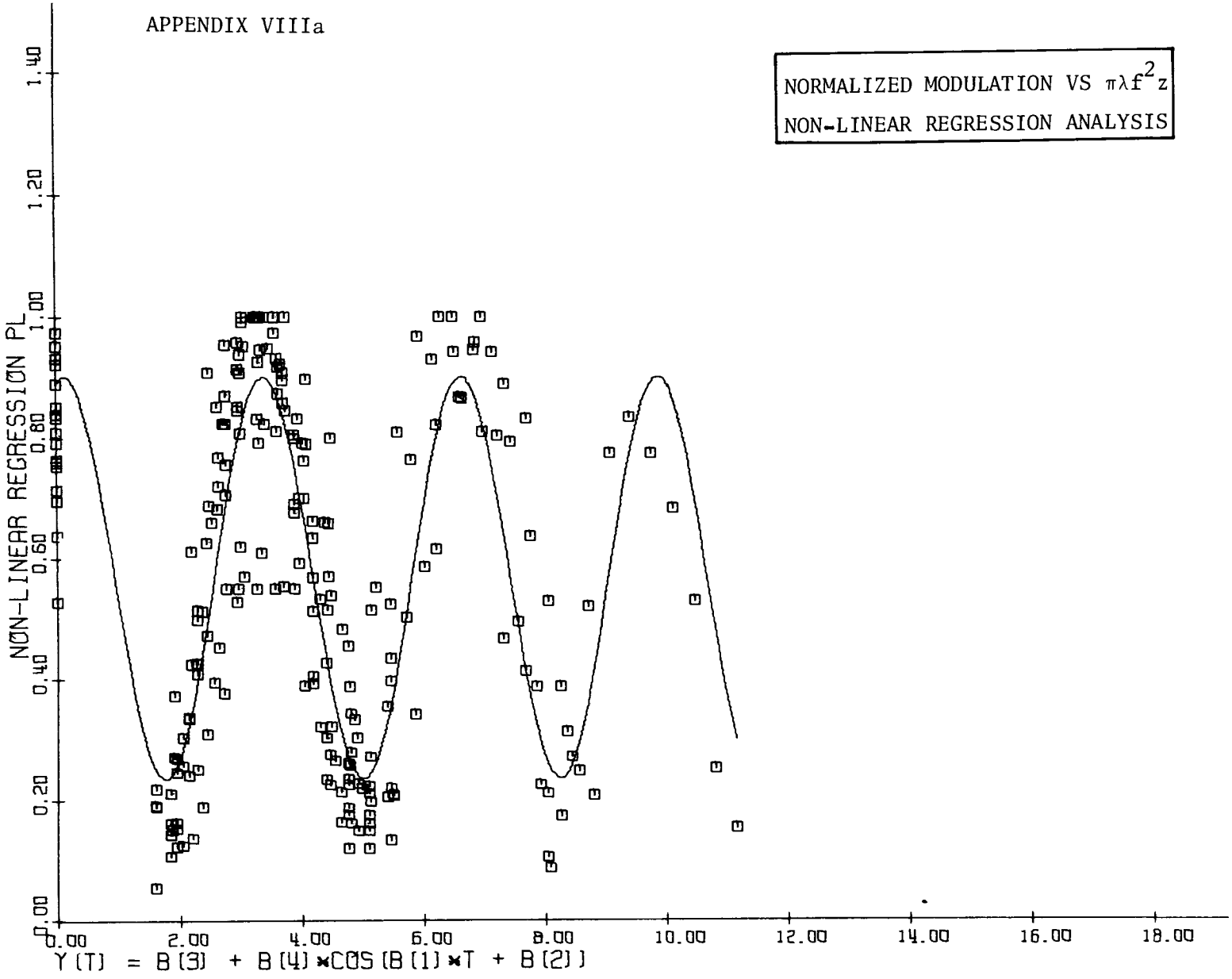

APPENDIX VIIIb